

# Multi-Resolution Signal Processing Techniques for Airborne Radar

Jameson S. Bergin, Christopher M. Teixeira, Paul M. Techau

Information Systems Laboratories, Inc.  
8130 Boone Blvd. ste. 500  
Vienna, VA 22182 USA

jsb@isl-inc.com, cmt@isl-inc.com, pmt@isl-inc.com

## ABSTRACT

*Synthetic aperture radar (SAR) exploits very high spatial resolution via temporal integration and ownship motion to reduce the background clutter power in a given resolution cell to allow detection of non-moving targets. Ground moving target indicator (GMTI) radar, on the other hand, employs much lower resolution processing, but exploits relative differences in the space-time response between moving targets and clutter for detection. Therefore, SAR and GMTI represent two different temporal processing resolution scales which have typically been optimized and demonstrated independently to work well for detecting either stationary (in the case of SAR) or exo-clutter (in the case of GMTI) targets.*

*Based on this multi-resolution interpretation of airborne radar data processing there appears to be an opportunity to develop detection techniques that attempt to optimize the signal processing resolution scale (e.g., length of temporal integration) to match the dynamics of a target of interest. This paper investigates signal processing techniques that exploit long CPIs to improve the detection performance of very slow moving targets.*

## 1. INTRODUCTION

A major goal of the KASSPER program is to develop new techniques for detecting and tracking slow-moving surface targets that exhibit maneuvers such as stops and starts. Therefore, it is logical to assume that a combination of SAR and GMTI processing may offer a solution to the problem. SAR exploits very high spatial resolu-

tion via temporal integration and ownship motion to reduce the background clutter power in a given resolution cell to allow detection of non-moving targets. GMTI radar, on the other hand, employs much lower resolution processing, but exploits relative differences in the space-time response between moving targets and clutter for detection. Therefore, SAR and GMTI represent two different temporal processing resolution scales which have typically been optimized and demonstrated independently to work well for detecting either stationary (in the case of SAR) or fast-moving (in the case of GMTI) targets.

Based on this multi-resolution interpretation of airborne radar data processing there appears to be an opportunity to develop detection techniques that attempt to optimize the signal processing resolution scale (e.g., length of temporal integration) to match the dynamics of a target of interest. For example, it may be beneficial to vary the signal processing algorithm as a function of Doppler shift (i.e., target radial velocity) such that SAR-like processing is used for very low Doppler bins, long coherent processing interval (CPI) GMTI processing is used for intermediate bins, and standard GMTI processing is used in the high Doppler bins. Figure 1 illustrates the concept. While not addressed in this paper, Figure 1 also suggests that varying the bandwidth as a function of target radial velocity may also be appropriate.

This paper explores signal processing techniques that “blur” the line between SAR and GMTI processing. We focus on STAP implementations using long GMTI CPIs as well as SAR-like processing strategies for detecting slow-moving targets. The performance of the techniques is demonstrated using ideal clutter covariance analysis as well as radar sample simulations

Section 2 presents the details about the radar simulation used to analyze the signal processing algorithms. Section 3 investigates the advantages of long CPIs using ideal covariance analysis. Section 4 introduces two

---

Presented at the 2003 KASSPER Workshop, Las Vegas, NV, 15-17 April, 2003.

This work was sponsored under Air Force Contract F30602-02-C-0005.

Approved for Public Release, Distribution Unlimited.

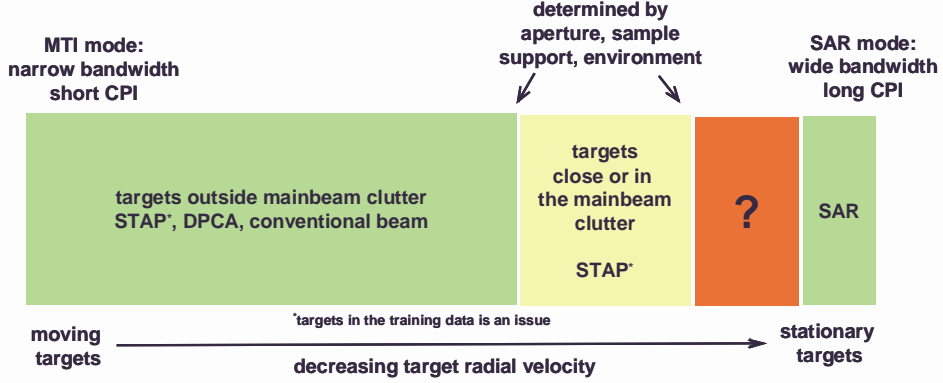


Fig. 1. Illustration of multi-resolution processing concept.

adaptive signal processing techniques that attempt to exploit the long CPIs to improve the detection performance of very slow moving targets. Section 5 presents performance results of the techniques using simulated radar samples. Finally, Section 6 summarizes the findings and outlines areas for further research.

## 2. GMTI RADAR SIMULATION

Simulated radar data was produced for use in analyzing the signal processing techniques proposed in this paper. Under previous simulation efforts [1-4] where the CPI length was short it was possible to ignore certain effects due to platform motion during a CPI (e.g., range-walk and bearing angle changes of the ground scattering patches). Under the current effort, however, where we are specifically interested in long CPIs it was important to produce simulated data that accurately accounts for the effects of platform motion. Therefore, the simulated data samples were computed as,

$$x(k, n, m) = \sum_{p=1}^{P_c} \alpha_p t_{p,m} s\left(kT_s - \frac{r_{p,m}}{c}\right) e^{j\left(\phi_n(\theta_{p,m}) - \frac{2\pi r_{p,m}}{\lambda}\right)}, \quad (1)$$

where  $k$  is the range bin index,  $m = 1, 2, \dots, M$  is the pulse index,  $n = 1, 2, \dots, N$  is the antenna index,  $N$  is the number of spatial channels,  $M$  is the number of pulses,  $s(t)$  is the radar waveform (LFM chirp compressed using a 30 dB sidelobe Chebychev taper),  $T_s$  is the sampling interval,  $\lambda$  is the radio wavelength,  $c$  is the speed of light,  $r_{p,m}$  and  $\theta_{p,m}$  are the two-way range and direction-of-arrival (DoA) respectively for the  $p^{th}$  ground clutter patch on the  $m^{th}$  pulse,  $\alpha_p$  is the complex ground scattering coefficient,  $\phi_n(\theta_{p,m})$  is the relative phase shift of the  $n^{th}$  antenna element for a signal from DoA  $\theta_{p,m}$ , and  $t_{p,m}$  is a random complex modulation from pulse to pulse due to internal clutter motion (ICM) [5].

The ideal clutter covariance matrix for a given range sample (i.e., range bin) is given as,

$$\mathbf{R}_k = \sum_{p=1}^{P_c} |\alpha_p|^2 \mathbf{v}_p \mathbf{v}_p^H \circ \mathbf{T}_{icm},$$

where the vector  $\mathbf{v}_p$  is the space-time response of the  $p^{th}$  scattering patch. The elements of  $\mathbf{v}_p$  are ordered such that the first  $N$  elements are the array spatial snapshot for the first pulse, the next  $N$  elements are the spatial snapshot for the second pulse, and so on. The elements of  $\mathbf{v}_p$  are given as,

$$v_p[N(m-1) + n] = s\left(kT_s - \frac{r_{p,m}}{c}\right) e^{j\left(\phi_n(\theta_{p,m}) - \frac{2\pi r_{p,m}}{\lambda}\right)},$$

Finally, we note that the matrix  $\mathbf{T}_{icm}$  is a covariance matrix taper [6] that accounts for the decorrelation among the pulses due to ICM and is based on the Billingsley spectral model for wind-blown foliage [7].

The simulation geometry is shown in Figure 2. The platform is flying north at an altitude of 11 km and the radar antenna is steered to look aft  $17^\circ$ . The clutter environment consists of an area at a slant range of 38 km that is slightly wider in the cross-range dimension than the antenna subarray pattern. The area is comprised of a grid of scattering patches of dimension 6 m x 6 m. The complex amplitudes of the scattering patches are i.i.d. Gaussian with zero mean and variance that results in a clutter-to-noise ratio for a single subarray and pulse of approximately 40 dB at the slant range of 38 km. A list of system parameters is given in Table 1.

We note that for this particular scenario that a given scattering patch in the mainbeam will “walk” on the order of one range resolution cell relative to the platform (due to platform motion) during the course of the 0.5 second CPI.

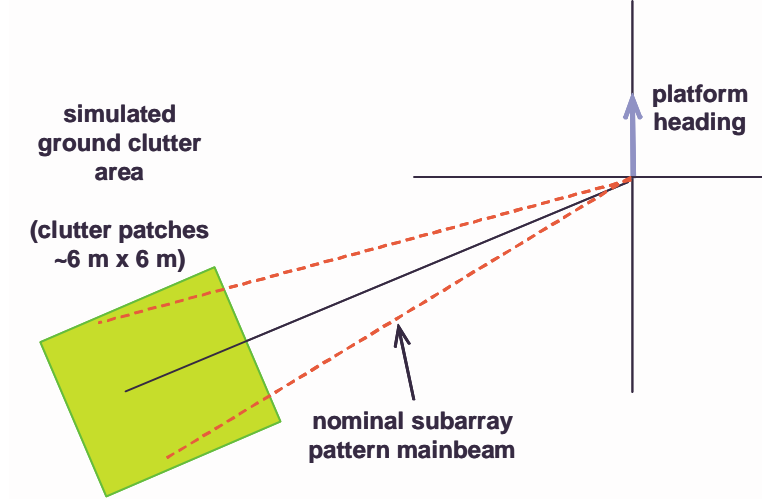


Fig. 2. Simulation geometry.

parameter	value (units)
frequency	X-band
bandwidth	10 MHz
PRF	1 kHz
number of pulses	512
antenna	3.5 m x 0.3 m
number of subarrays	6 (50% overlap)
subarray pattern	Hamming (~40 dB sidelobes)
CNR	40 dB per subarray/pulse
platform speed	125 m/s
azimuth steering direction	17° re. broadside

Table 1. simulation parameters

### 3. IDEAL COVARIANCE ANALYSIS

This section presents the results of GMTI system performance analyses as a function of CPI length using the ideal ground clutter covariance matrix.

#### 3.1. Ground Clutter Cancellation

The ideal clutter covariance was used to investigate GMTI performance as a function of the CPI length using optimal space-time beamforming. The goal of this analysis was to help establish an understanding of the theoretical advantages of using longer CPIs to detect moving targets. We employed a multi-bin post-Doppler space-time beamformer [8] with weights computed using the ideal clutter plus thermal noise covariance matrix,

$$\mathbf{w}_o(\theta, f_d) = (\mathbf{H}^H(\mathbf{R}_k + \mathbf{R}_n)\mathbf{H})^{-1}\mathbf{H}^H\mathbf{v}(\theta, f_d) \quad (2)$$

where  $\mathbf{H}$  is a matrix that transforms to post-Doppler element space (i.e., each column of  $\mathbf{H}$  represents one of the

adjacent Doppler filters),  $\mathbf{R}_n$  is the covariance of the thermal noise, and  $\mathbf{v}(\theta, f_d)$  is the space-time response of a signal with DoA  $\theta$  and Doppler shift  $f_d$ . We note that  $\mathbf{v}(\theta, f_d)$  is the usual space-time steering vector [9] and does not include the effects of range-walk. Also, in the SINR results we do not account for the small losses that this will cause due to mismatch with a true target response.

Figure 3 shows the signal-to-interference plus noise ratio (SINR) loss as a function of CPI length for the cases with and without ICM. SINR loss is defined as the system sensitivity loss relative to the performance in an interference-free environment [9]. In this case we have used 7 adjacent Doppler bins formed via orthogonal Doppler filters. It was found that using more Doppler bins resulted in negligible gain in performance. It is interesting to note that the shape of the filter response versus Doppler does not improve significantly as the CPI length is increased suggesting that the gains in minimum detectable velocity will be modest for longer CPIs.

Figure 4 shows the SINR for the two cases shown in Figure 3 relative to the 8 pulse case. Thus we see the effects of the increased sensitivity gain achieved by using more pulses (i.e., longer integration time). If we assume that the SINR for the 8 pulse case is 17 dB in the Doppler bins well-separated from the clutter ridge then the MDV point will be at approximately -5 dB on the SINR loss curve (i.e., SINR = 12 dB which is a nominal detection threshold). Therefore since the curves in Figure 4 are relative to the 8 pulse case the MDV point for each CPI will also occur at -5 dB.

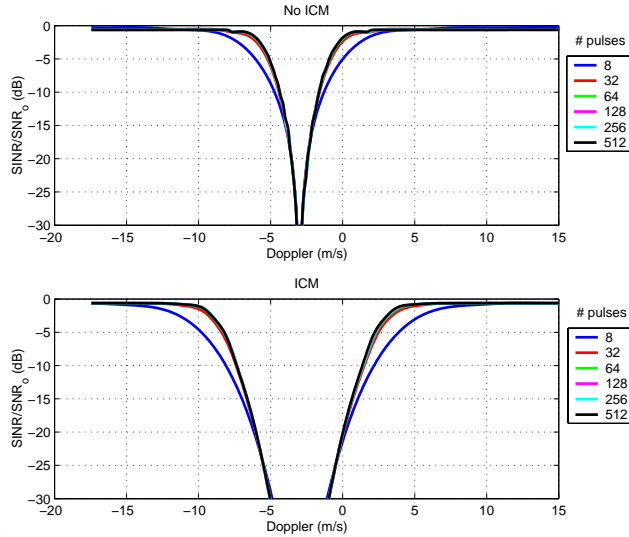


Fig. 3. Optimal SINR loss. Top: no ICM. Bottom: Billingsley ICM. The center of the clutter notch is at -3 m/s (two-way Doppler).

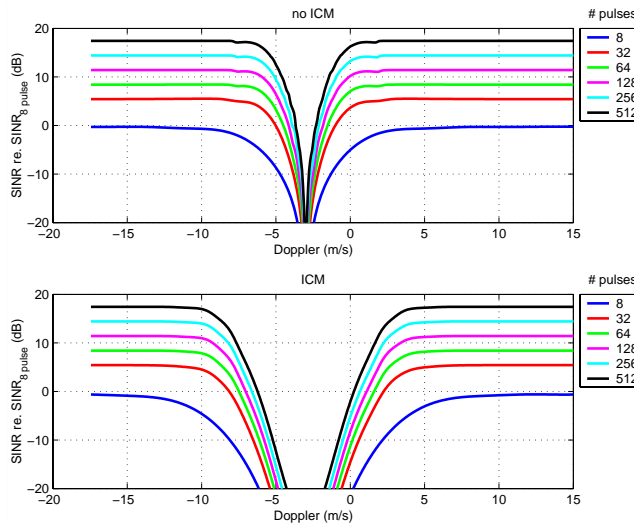


Fig. 4. Optimal SINR re. 8 pulse case. Top: no ICM. Bottom: Billingsley ICM.

Figure 5 plots the MDV value as a function of the CPI length for the cases with and without ICM. We see that the gain in MDV drops off rapidly as the CPI length is increased. Therefore, we conclude that arbitrarily increasing the CPI will not result in significant gains in MDV beyond a certain point which will generally be determined by the system aperture size and ICM (or other sources of random modulations from pulse-to-pulse)

### 3.2. Targets in the Secondary Training Data

While longer CPIs do not significantly improve the ability to resolve targets from clutter beyond a certain point due to the distributed Doppler response of ground

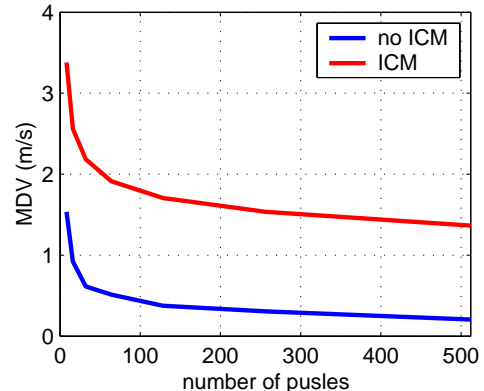


Fig. 5. MDV based on the curves shown in Figure 4.

clutter as observed by a moving airborne platform there is the potential that longer CPIs will help better resolve targets in the scene. This has the obvious benefits of improving tracker performance by allowing clusters of closely-spaced targets to be resolved.

An even greater potential benefit of the improved ability to resolve targets is that targets corrupting the secondary training data [3,10] will be less likely to result in losses on other nearby targets. This is illustrated in Figure 6 where the SINR loss is shown for the case when a single target is injected into the ideal clutter covariance with a Doppler shift of 4.8 m/s. We see that as the CPI length is increased the region incurring losses due to the target in the covariance gets increasingly narrow indicating that it will only take a very small relative Doppler offset between two targets to avoid them from canceling one another. Quantifying the effectiveness of longer CPIs in mitigating the problem of targets in the secondary training data for *realistic* moving target scenarios is an area for future research.

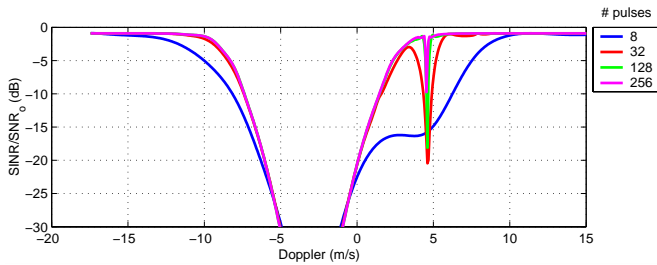


Fig. 6. Optimal SINR loss for the case when a single target corrupts the secondary training data. The target corrupting the training data has Doppler = 4.8 m/s.

#### 4. ADAPTIVE ALGORITHMS

This section proposes two adaptive signal processing algorithms that exploit long CPIs to improve the detection performance of very slow-moving targets. The goal will be to evaluate the hypothesis that longer CPI data may be exploited to increase the number of samples available for covariance estimation without significantly increasing the range swath over which samples are drawn. It is assumed that this will be advantageous in realistic clutter environments where variations in the terrain and land cover often limit the stationarity of the radar data in the range dimension to narrow regions.

##### 4.1. Sub-CPI Processing

The ideal covariance analysis presented in Section 3.1 suggests that for a given system it may not be necessary to coherently process all the pulses in a long CPI to approach the optimal MDV. Therefore, if many pulses

are available it may be advantageous to limit the coherent processing interval, but exploit the extra pulses to increase the training data set for covariance estimation. It is important to note that the potential advantage of reducing effects due to targets in the training data will not be realized in this case since the *coherent* processing interval is still short. For example, Figure 7 illustrates an approach for segmenting the pulses to form data snapshots that can be used for covariance estimation. In this case the sample covariance matrix is computed as,

$$\hat{\mathbf{R}} = \frac{1}{K + K'} \sum_{k=1}^K \sum_{k'=1}^{K'} \mathbf{x}_{k,k'} \mathbf{x}_{k,k'}^H$$

where  $\mathbf{x}_{k,k'}$  is the snapshot from the  $k^{\text{th}}$  range bin and  $k'^{\text{th}}$  sub-CPI. We note that vector  $\mathbf{x}_{k,k'}$  is formed by reordering the matrix  $\mathbf{X}_{k,k'}$  shown in Figure 7 so that the first  $N$  elements are the spatial samples on the first pulse, the next  $N$  elements are the spatial samples on the second pulse, and so on. The quantity  $K$  is the number of training range samples and  $K'$  is the number of sub-CPIs used in the training. The effect of varying these quantities is demonstrated in Section 5.

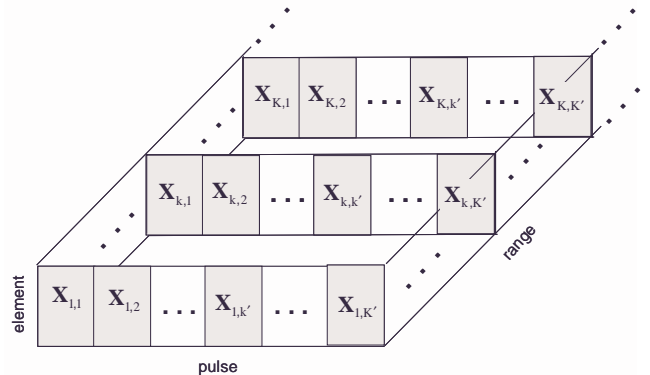


Fig. 7. Illustration of sub-CPI segmentation.

The covariance estimate based on the sub-CPI data is used to compute an adaptive weight vector that can generally be applied to each of the sub-CPIs in the range bin under test to form  $K'$  complex beamformer outputs. Methods for combining these outputs either coherently or incoherently to improve the system sensitivity is an area for future research. It is worth noting, however, that in general it should be possible to coherently combine the outputs if unity gain constraints are employed in the beamformer calculation and delays in the target response in each sub-CPI relative to the start of the CPI are accounted for.

## 4.2. Long-CPI Post-Doppler

An alternative approach to sub-CPI processing is to Doppler process (e.g. discrete Fourier transform) the CPI using all the pulses and then apply adaptive techniques similar to multi-bin post Doppler STAP [8]. In the case when the CPI is very long it may be advantageous to employ SAR processing instead of Doppler processing which will account for range-walk of the scattering elements in the scene due to platform motion. This approach has been proposed previously [11]. Figure 8 illustrates the concept. We note that this technique will take advantage of the property of long CPIs to reduce the effects of targets in the secondary training data as long as multiple adaptive Doppler bins are employed.

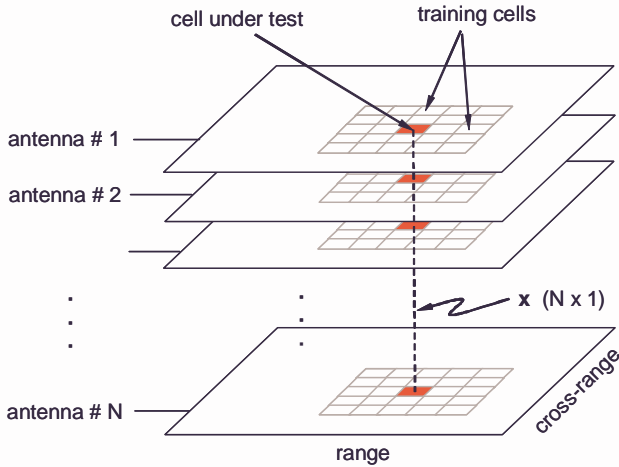


Fig. 8. Illustration of long-CPI post Doppler processing. Note training is possible in both range and cross-range.

In the simplest form the data from each antenna is used to form a spatial-only covariance estimate using data from Doppler and range bins (or cross-range and range pixels in the case of SAR pre-processing). If we only employ data from adjacent range bins for training this technique (in the case of Doppler processing) is identical to factored time-space beamforming [9] (i.e., single bin post-Doppler adaptive processing). In [11] it was proposed that adjacent cross-range (or Doppler bins) should also be included in the training set. This may at first seem unusual in the context of GMTI STAP for which training using only adjacent range bins is the common practice.

Figure 9 illustrates why it is efficacious to use data from adjacent Doppler bins to estimate the correlation among the spatial channels when the CPI is long. We see that since the Doppler resolution is much finer than the

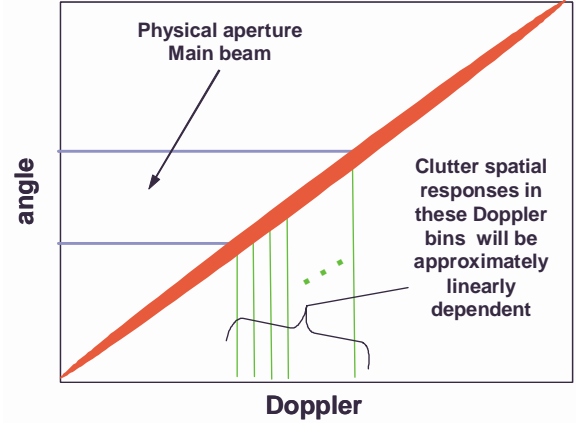


Fig. 9. Illustration of clutter ridge and large difference in angular and temporal resolution for long CPIs

spatial resolution that clutter patches in adjacent Doppler bins will have highly linearly dependent spatial responses and therefore can be averaged to improve the spatial covariance estimate<sup>1</sup>. The azimuth beamwidth of the physical aperture is given as,

$$\delta_a = \frac{\lambda}{L},$$

where  $L$  is the length of the aperture in the horizontal dimension. The azimuth beamwidth of the synthetic aperture (azimuthal extent of the ground clutter in a single Doppler bin) is given as [12],

$$\delta_d = \frac{\lambda}{2L_{eff}} = \frac{\lambda f_p}{2v_p M},$$

where  $L_{eff}$  is the distance traveled by the platform during the CPI,  $f_p$  is the PRF, and  $v_p$  is the platform speed. The ratio of  $\delta_a$  to  $\delta_d$ ,

$$f_{res} = \frac{\delta_a}{\delta_d} = \frac{2v_p M}{L f_p},$$

gives an approximate expression for the number of Doppler bins within the mainbeam and thus the number of adjacent Doppler bins that can be used as training samples. For the system simulation discussed in Section 2 the quantity  $f_{res} = 37.4$ .

Figure 10 demonstrates the effects of increasing the number of adjacent Doppler bins used in the training set for the single adaptive bin case (i.e., factored time-space adaptive beamforming). The total number of pulses in

<sup>1</sup>To our knowledge this is the first time an attempt has been made to theoretically explain in the open literature the concept of using adjacent Doppler bins for spatial covariance training when the CPI is long.

the CPI is 256 which results in  $f_{res} = 18.7$  and we note that a 65 dB sidelobe level Chebychev taper is applied across the 256 pulses prior to Doppler processing. In this example the ideal spatial-only covariance matrix for each of the adjacent Doppler bins used in the training strategy was computed and then summed together to form the ‘ideal’ estimated covariance. This covariance, which takes into account the effects of training over adjacent Doppler bins, was then used to compute SINR loss. As expected, when the number of bins exceeds about  $f_{res} = 18.7$  the SINR loss begins to degrade appreciably.

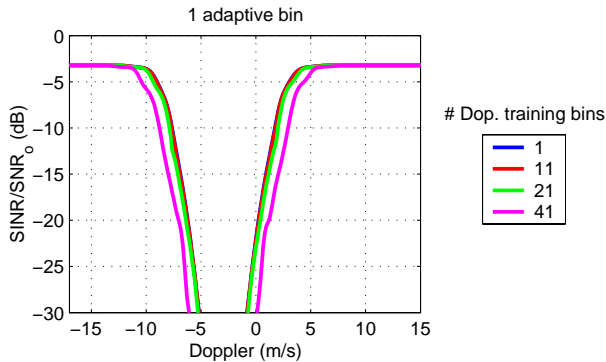


Fig. 10. Effect of Doppler training region size in long CPI post-Doppler processing. The training bins are centered around and include the bin under test.

More sophisticated versions of the long-CPI post-Doppler algorithm will include multiple temporal degrees of freedom. In [11] multiple adjacent SAR pixels were combined adaptively along with the spatial channels to form the adaptive clutter filter. When training samples are only chosen from adjacent range bins this version of the algorithm is similar to multi-bin post-Doppler element space STAP [8]. In fact, if the pre-processing uses Doppler filters instead of SAR processing the algorithm is mathematically equivalent to multi-bin post-Doppler STAP.

Choosing training samples from adjacent Doppler and range bins is not as straight forward as it was in the single adaptive bin case since the samples can be chosen to be either overlapped or non-overlapped in Doppler. In [11] it was observed that the multi-pixel covariance estimation process introduced ‘‘artificial’’ increases in the correlation of the background thermal noise between pixels when the overlapped training samples were used since the thermal noise for two overlapping training samples will typically be correlated. Theoretical analysis of estimators that use overlapping training data to

estimate the multi-pixel correlation matrix is an area for future research.

## 5. RESULTS

The simulated data discussed in Section 2 was used to test the two long CPI adaptive processing techniques proposed in this paper. Five range samples were simulated and an ideal covariance matrix for the center range bin was generated. Adaptive weights were estimated from the data samples using the various training strategies and then combined with the ideal covariance matrix to compute the SINR loss metric.

Figure 11 shows the SINR loss for sub-CPI processing as a function of the number of pulses in the sub-CPI for three cases 1) range-only training, 2) sub-CPI only training, and 3) range and sub-CPI training. The adaptive algorithm was multi-bin post-Doppler element space STAP employing 3 adjacent adaptive Doppler bins. Diagonal loading with a level of 0 dB relative to the thermal noise was used in all cases.

We see that range-only training results in poor performance since there are too few training samples to support the adaptive DoFs. Performance is improved by alternatively using the sub-CPIs from a single range bin as the training data. In this case the number of training samples is equal to the total number of pulses (512) divided by the number of pulses in the sub-CPI. Thus for the examples shown the number of sub-CPI training samples is 64, 32, and 16 for the 8, 16, and 32 pulse sub-CPI cases respectively.

Finally, we see that if training samples are chosen from both sub-CPIs and range bins we get near-optimal (relative to the ideal covariance case) performance. In this case the total number of training samples is the number of range bins multiplied by the number of sub-CPI segments. Thus the number of samples for the cases shown is 320, 160, and 80 for the 8, 16, and 32 pulse sub-CPI cases respectively. This example demonstrates that highly localized training regions in range may be possible if training data is augmented with sub-CPI data snapshots. This strategy will generally be the most advantageous in nonhomogeneous clutter environments.

Figure 12 shows the SINR loss results for the long-CPI post-Doppler processing technique. The results are presented for three cases 1) a single adaptive Doppler bin, 2) 3 adjacent adaptive Doppler bins with *overlapped* Doppler training snapshots, and 3) 3 adjacent adaptive Doppler bins with *non-overlapped* Doppler training snapshots. In each case the CPI length is 512 and training data from 21 adjacent Doppler filters is used in the covariance estimation. In this case

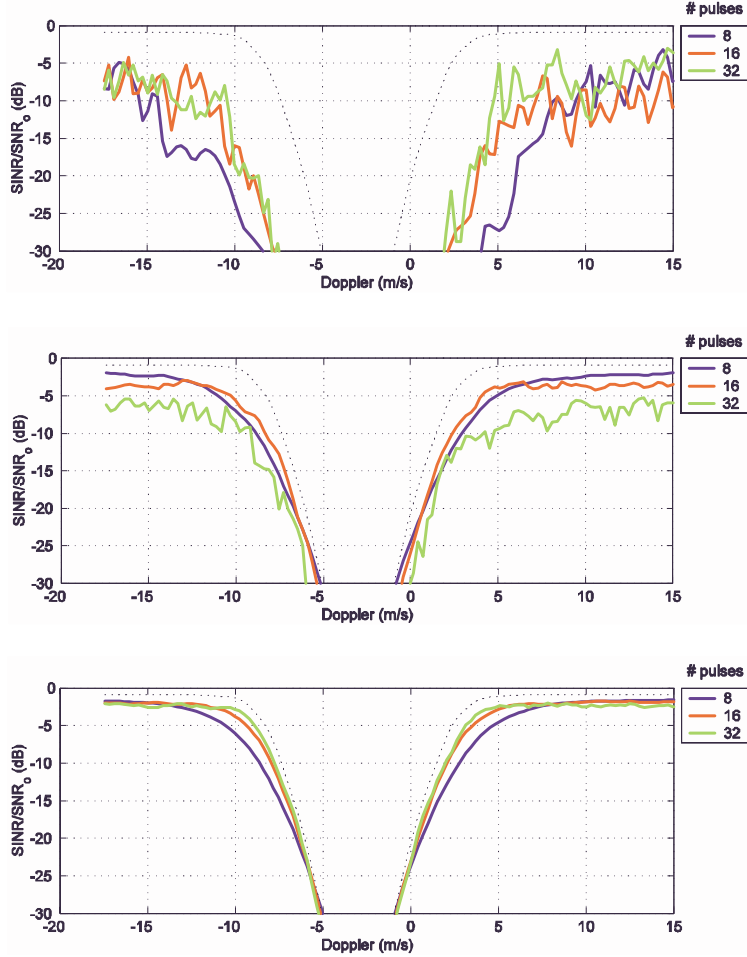


Fig. 11. SINR loss for sub-CPI training. Top: range-only training (5 range bins). Middle: training using sub-CPIs from a single range bin. Bottom: training using sub-CPIs from 5 range bins. The black dotted line is optimal full-DoF STAP performance.

$f_{res} = 34.7$ , but a value of 21 was used to ensure that no losses were incurred due to over-extending the Doppler training window. We also note that the single adaptive Doppler bin case employs a 65 dB sidelobe level Chebyshev taper across the 512 pulses prior to Doppler processing.

The upper left hand plot (‘1 adaptive bin’) has a black dashed curve which represents the case when 5 range samples are used to estimate the spatial covariance matrix which in this case has dimension 6 due to the 6 spatial channels employed in the simulation. We note that diagonal loading at a level of 0dB relative to the thermal noise floor was required so the estimated covariance matrix could be inverted. We see that the range-only training results in poor performance due to the small number of training samples.

We see, however, that when adjacent Doppler bins are used for training we get much better performance (red and green curves). The red curve uses adjacent Doppler

bins and 5 range samples for training data and the green curve uses adjacent Doppler bins from a single range bin. We see that the best performance is achieved when multiple adaptive Doppler bins are employed and training is performed using both adjacent range bins and overlapping Doppler samples. The generally poor performance when only adjacent Doppler samples are used is most likely attributed to the correlation of the thermal noise among the training samples which results in a poor estimate of the background thermal noise statistics. Developing a better understanding of this phenomenon via analysis and simulation is an area for future research.

## 6. CONCLUSIONS

The concept of using long CPIs to improve the detection of very slow-moving targets was investigated. The concept was motivated by observing that airborne radars use short CPIs to detect fast moving targets (e.g., GMTI STAP) and very long CPIs to detect stationary targets

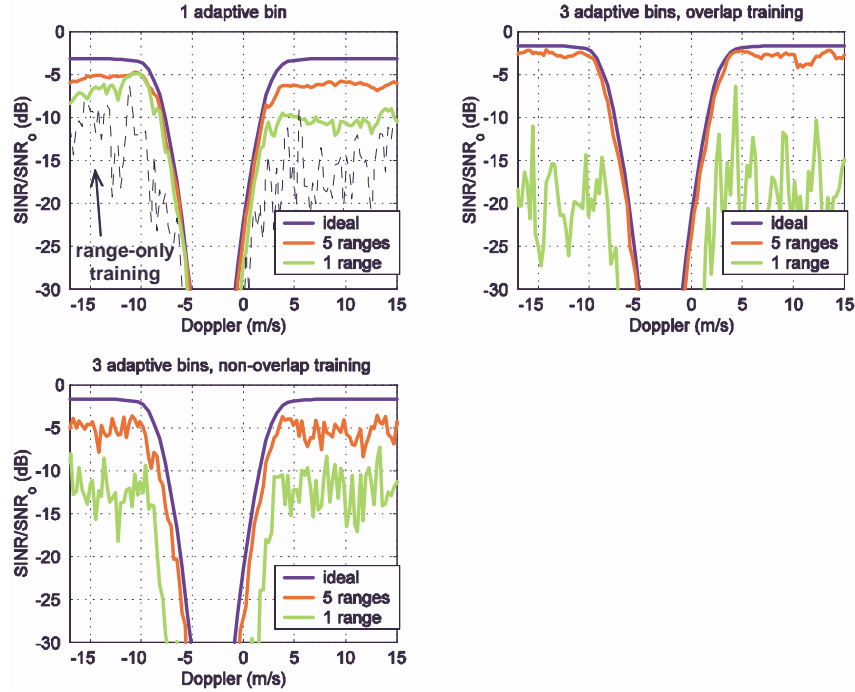


Fig. 12. Long CPI post-Doppler processing. Top left: one adaptive bin (factored post-Doppler). Top right: 3 adaptive bins (multi-bin post-Doppler) with *overlapped* training. Bottom left: 3 adaptive bins with *non-overlapped* training. Red and Green curves are for adjacent Doppler bin training strategy using either a single (green) or five (red) range samples.

(e.g., SAR) so that it is logical to assume that it may be advantageous to use longer and longer CPIs as the assumed Doppler velocity of targets of interest is decreased.

Theoretical analysis of optimal beamforming techniques that cancel clutter (e.g., STAP) was used to demonstrate that for a given system and operating environment that there is a CPI length beyond which significant improvements in MDV diminish. Beyond the cut-off the width of the antenna and phenomenology such as ICM limit the MDV performance. It was postulated, however, that the problem of targets corrupting the training data may be significantly reduced since when the CPI is long it will require only a very small relative difference in Doppler velocity between targets to cause enough decorrelation so that when they corrupt the training data the resulting sensitivity losses are negligible.

While the improvements of optimal beamformers in detecting very slow moving targets tends to diminish beyond a certain CPI length *adaptive* implementations of the optimal beamformers may benefit significantly from longer CPIs. Two adaptive techniques were presented that take advantage of the longer CPI to improve the convergence properties of the beamformer solution and thus increase the performance of the beamformer. It

was shown that these techniques can reduce the number of adjacent range samples required for training which will generally improve performance in realistic clutter environments where the stationarity of the ground clutter is often limited to narrow range regions due to significant terrain relief and land cover variations.

The proposed algorithms were tested using a homogeneous clutter simulation that represents a nominal X-band GMTI radar system. Future work is required to determine the performance of the proposed techniques in more realistic clutter environments and for varying system parameters such as larger scanning angles and higher bandwidths. The goal of the future work will be to develop a better theoretical understanding of the techniques via analysis and simulation and to determine under what operating conditions and for what types of systems they are best suited.

Finally, other approaches to multi-resolution processing will be pursued. The concept of optimizing the radar resources (i.e., CPI length and bandwidth) to improve detection performance as a function of assumed target Doppler shift is an area that may lead to radar systems with significantly improved ability to track ground targets.

## 7. REFERENCES

- [1] J. S. Bergin and P. M. Techau, "High fidelity site-specific radar simulation: KASSPER '02 Workshop datacube," ISL Tech. Report ISL-SCRD-TR-02-105, May, 2002.
- [2] J. S. Bergin and P. M. Techau, "High-Fidelity Site-Specific Radar Simulation: KASSPER Data Set 2," ISL Technical Report, ISL-SCRD-TR-02-106, October, 2002, Vienna, VA.
- [3] J. S. Bergin, P. M. Techau, W. L. Melvin, and J. R. Guerci, "GMTI STAP in target-rich environments: site-specific analysis," *Proceedings of the 2002 IEEE Radar Conference*, Long Beach, CA, 22-25, April 2002.
- [4] P. M. Techau, J. R. Guerci, T. H. Slocumb, and L. J. Griffiths, "Performance bounds for hot and cold clutter mitigation," *IEEE Transactions on Aerospace and Electronic Systems*, vol. 35, pp. 1253-1265, October, 1999.
- [5] J. B. Billingsley, "Exponential decay in windblown radar ground clutter Doppler spectra: multifrequency measurements and model," Technical Report 997, MIT Lincoln Laboratory, Lexington, MA, July 29, 1996.
- [6] J. R. Guerci, "Theory and application of covariance matrix tapers for robust adaptive beamforming," *IEEE Transactions on Signal Processing*, vol. 47, pp. 997-985, April, 1999.
- [7] P. M. Techau, J. S. Bergin, and J. R. Guerci, "Effects of internal clutter motion on STAP in a heterogeneous environment", *Proceedings of the 2001 IEEE Radar Conference*, Atlanta, GA, pp. 204 -209, 1-3 May 2001.
- [8] R. C. DiPietro, "Extended factored space-time processing for airborne radar systems," *Record of the Twenty-Sixth Asilomar Conf. on Signals, Systems and Computers*, vol. 1, pp. 425-430, October 26-28, 1992.
- [9] J. Ward, "Space-time adaptive processing for airborne radar," Lincoln Laboratory, Tech. Report 1015, December, 1994.
- [10] W. L. Melvin and J. R. Guerci, "Adaptive detection in dense target environments," *Proceedings of the 2001 IEEE Radar Conference*, Atlanta, GA, pp. 187-192, 1-3 May 2001.
- [11] A. Yegulalp, "FOPEN GMTI using multi-channel adaptive SAR," *Proceedings of the Tenth Annual Adaptive Sensor Array Processing Workshop*, MIT Lincoln Laboratory, Lexington, MA, 12-14 March 2002.
- [12] M. Skolnik, *Radar Handbook*, McGraw Hill, Boston, MA, 1990